Earth and Planetary Science Letters 556 (2021) 116707

Contents lists available at ScienceDirect

Earth and Planetary Science Letters

www.elsevier.com/locate/epsl

Nitrogen and noble gases reveal a complex history of metasomatism in the Siberian lithospheric mantle

Peter H. Barry [a,*], Michael W. Broadley [b]

[a] Woods Hole Oceanographic Institution, MC&G Dept., Woods Hole, MA, 02543, USA
[b] Centre de Recherches Pétrographiques et Géochimiques, Université de Lorraine, Nancy, France

ARTICLE INFO

Article history:
Received 5 October 2020
Received in revised form 21 November 2020
Accepted 3 December 2020
Available online 24 December 2020
Editor: R. Dasgupta

Keywords:
nitrogen
neon
argon
SCLM
metasomatism
plume

ABSTRACT

The Siberian flood basalts (SFB) erupted at the end of the Permian period (~250 Ma) in response to a deep-rooted mantle plume beneath the Siberian Sub-Continental Lithospheric Mantle (SCLM). Plume-lithosphere interaction can lead to significant changes in the structure and chemistry of the SCLM and trigger the release of metasomatic material that was previously stored within the stable craton. Here, we investigate the nature of the Siberian-SCLM (S-SCLM) by measuring nitrogen abundances and isotopes (δ^{15}N) in 11 samples of two petrologically-distinct suites of peridotitic xenoliths recovered from kimberlites which bracket the eruption of the SFB: the 360 Myr old Udachnaya and 160 Myr old Obnazhennaya pipes. Nitrogen isotope (δ^{15}N) values range from -5.85 ± 1.29‰ to +3.94 ± 0.63‰, which encompasses the entire range between depleted Mid-Ocean Ridge Basalt (MORB) mantle (DMM; -5 ± 2‰) and plume-derived (+3 ± 2‰) endmembers. In addition, we present neon (n=7) and argon (n=8) abundance and isotope results for the same two suites of samples. The ^{20}Ne/^{22}Ne and ^{21}Ne/^{22}Ne range from atmospheric-like values of 9.88 up to 11.35 and from 0.0303 to 0.0385, respectively, suggesting an admixture of DMM and plume-derived components. Argon isotopes (^{40}Ar/^{36}Ar) range from 336.7 to 1122 and correlate positively with ^{40}Ar contents. We show that volatile systematics of Siberian xenoliths: (1) exhibit evidence of ancient metasomatic and/or recycled signatures, and (2) show evidence of subsequent plume-like re-fertilization, which we attribute to the emplacement of the SFB. Metasomatic fluids are highly enriched in radiogenic gases and have elevated Br/Cl and I/Cl values, consistent with an ancient subducted crustal component. The metasomatic component is marked by light N isotope signatures, suggesting it may be derived from an anoxic Archean subducted source. Taken together, these N_2-Ne-Ar isotope results suggest that mantle plume impingement has profoundly modified the S-SCLM, and that N, Ne and Ar isotopes are sensitive tracers of metasomatism in the S-SCLM. Metasomatic fluids that permeate the S-SCLM act to archive a "subduction-fingerprint" that can be used to probe relative volatile-element recycling efficiencies and thus provide insight into volatile transport between the surface and mantle reservoirs over Earth history.

1. Introduction

The SCLM, which formed through the repeated under-thrusting of oceanic slabs beneath stable continental crust (Griffin and O'Reilly, 2007), represents a relatively minor component of the Earth's depleted mantle (~ 1.5 vol%). It has remained isolated from the convecting asthenosphere over billion-year time-scales (Pernet-Fisher et al., 2015) and now forms the interface between the mantle and the stable continental crust. Due to its isolation from the convecting mantle, the SCLM has retained local geochemical heterogeneities introduced through interactions with mantle-plumes, crustal and/or subduction-related sources since its formation. The SCLM therefore represents a potentially important geological reservoir where energy and mass fluxes are greatly-enhanced and focused, acting as magnifying lenses into metal and volatile transport fractionation, ultimately leading to ore deposition (Holwell et al., 2019). The ability of the SCLM to retain metasomatic components over geologically-significant periods of time indicates that it could potentially constitute a significant long-term reservoir of volatile elements (Broadley et al., 2018a). Furthermore, the release of volatiles stored in the SCLM to the surface during thermal events associated with plume impingement and rifting could have globally-significant effects on the environment, which further highlights the importance of understanding the contribution of the

* Corresponding author.
E-mail address: pbarry@whoi.edu (P.H. Barry).

https://doi.org/10.1016/j.epsl.2020.116707
0012-821X/

SCLM to the global volatile budget (Broadley et al., 2018a). This is particularly the case for S-SCLM, where the thick stable cratonic lithosphere may have accumulated significant quantities of metasomatic volatiles over billions of years (Broadley et al., 2018a).

Isotopic and elemental signatures of volatiles such as nitrogen, noble gas and halogens can be used to quantify the extent of metasomatic modification and potentially reveal important information about the source(s) of volatiles within the SCLM. Coupled noble gas and halogen studies have been used in the past to suggest that a significant proportion of volatiles in the mantle may have been introduced by the subduction of marine pore fluids, serpentinites and altered oceanic crust (AOC) (Sumino et al., 2010; Kendrick et al., 2011; Chavrit et al., 2016; Broadley et al., 2016). Mantle xenoliths sourced from the SCLM contain volatiles hosted in self-contained fluid inclusions that are unlikely to be contaminated by surface components. They can therefore provide a direct window into the volatile composition of the SCLM. From the analysis of SCLM xenoliths, it has been suggested that the volatiles trapped in the SCLM may also originate from surface-derived metasomatic fluids (e.g., Broadley et al., 2016) that were introduced during periods of subduction and went on to pervasively modify the composition of the SCLM.

Geochemical investigations of N isotopes in various terrestrial reservoirs have revealed a discernible N isotopic contrast between surface reservoirs and the mantle. For example, the DMM is estimated to have a δ^{15}N of $\sim$ -5 $\pm$ 2‰ (Javoy et al., 1986; Marty and Zimmermann, 1999) (normalized to air, $\delta^{15}N_{air} = 0$‰). In contrast, the deep mantle, as sampled by the Kola magmatic province, Iceland, Yellowstone, Loihi Seamount, Hawaii and the Society Islands, is enriched in ^{15}N relative to air by up to +12‰ (Dauphas and Marty, 1999; Halldórsson et al., 2016; Labidi et al., 2020), with a mean δ^{15}N value of +3 $\pm$ 2‰. Modern ocean floor sediments are also enriched in ^{15}N, with δ^{15}N values ranging from +5 to +7‰ (e.g., Peters et al., 1978), indicating that high δ^{15}N material may be recycled into the deep mantle by modern subduction processes (Barry and Hilton, 2016; Bekaert et al., 2021). Nitrogen isotopes may therefore be able to provide a new insight into the origin of volatiles in the SCLM.

Despite a number of studies over the past two decades (e.g., Matsumoto et al., 2002; Yokochi et al., 2009; Yamamoto et al., 2020), the nitrogen isotope composition of SCLM remains poorly constrained. Several investigations of N and Ar in peridotitic fluid inclusions showed δ^{15}N values similar to those of oceanic basalts (Yamamoto et al., 2020), with slightly higher N_2/Ar values, attributed to recycled crustal material (Matsumoto et al., 2002). The S-SCLM beneath Udachnaya is one of the most geochemically well-characterized sections of the S-SCLM (e.g., Pokhilenko et al., 1999; Sumino et al., 2006). However, to date, relatively few studies have investigated the origin of the metasomatic processes responsible for the compositional variations reported in associated peridotites (e.g., Pokhilenko et al., 1999; Howarth et al., 2014; Barry et al., 2015; Pernet-Fisher et al., 2015, 2019; Broadley et al., 2018a). Here we use Ne-N-Ar isotopes and halogen elemental ratios in order to identify the different volatile components present in the S-SCLM. This multi-tracer approach provides unique insights into the geochemical composition of the S-SCLM and enables the history of volatile interaction, potentially dating back to the Archean, to be determined.

2. Geologic settings

Cratonic areas represent ideal settings for studying the temporal evolution of the SCLM. The Siberian craton (see Fig. 1 in Barry et al., 2015) encompasses approximately 4.4 $\times$ 10^6 km^2 of north-central Asia. It is composed of several island-arc terrains, which amalgamated during the Archean and Proterozoic (Pearson et al., 1995), and has subsequently experienced a complex history of Phanerozoic metasomatism and kimberlite emplacement (e.g., Pearson et al., 1995; Griffin et al., 1999). Between the Silurian and Jurassic periods (Howarth et al., 2014), over 1000 kimberlites were intruded within Siberia (Griffin et al., 1999; Pokhilenko et al., 1999), transporting mantle xenolith material which had largely remained isolated from asthenospheric convection, to the Earth's surface.

Superimposed atop the Siberian craton is one of Earth's largest igneous provinces – the Siberian Flood Basalts (SFB) – which erupted $\sim$ 2 x 10^6 km^3 of basaltic magma over a 1-2 Myr duration at $\sim$250 Ma (Reichow et al., 2002; Kamo et al., 2003). Several independent lines of evidence, including thermal anomaly constraints (e.g., Sharapov et al., 2008) and plume-like He isotope data (Basu et al., 1995), suggest that SFB emplacement is directly related to the presence of a deep-rooted mantle plume beneath Siberia. Due to the close proximity of the SFB to the Siberian craton, it has been suggested that this large emplacement event modified the S-SCLM and vice versa (Sobolev et al., 2011; Broadley et al., 2018a).

Here, we focus on petrologically-distinct peridotite xenoliths (Howarth et al., 2014), which were transported to the surface by two Siberian kimberlites: the diamondiferous Late-Devonian Udachnaya (360 Ma) and Jurassic Obnazhennaya (160 Ma) pipes. As these eruptions bracket the $\sim$250 Myr old SFB event (Reichow et al., 2002), they provide insight into the Phanerozoic metasomatic history of the S-SCLM.

3. Results

3.1. Nitrogen abundances and isotopes

The δ^{15}N (where $\delta^{15}N = [(^{15}N^{14}N/^{14}N^{14}N)_{sample}/(^{15}N^{14}N/^{14}N^{14}N)_{air} - 1] \times 1000$) determined for the Siberian peridotite xenolith samples range between -5.85 and +3.94‰ relative to air (i.e., 0‰) (Table 1). Obnazhennaya samples (n=6) are ^{15}N-depleted, with δ^{15}N values ranging from -0.71 to -3.12‰ (Fig. 1; Table 1), which notably fall above the DMM range (Marty and Zimmermann, 1999; Cartigny and Marty, 2013). In contrast, Udachnaya samples (n=5) span the range from DDM to plume-like δ^{15}N (Fig. 1), with values from -5.85 to +3.94‰. N_2 contents extend from 5.20 to 36.0 µcm^3 STP N_2/g for Obnazhennaya samples and from 10.5 to 109 µcm^3 STP N_2/g for Udachnaya samples.

3.2. Neon abundances and isotopes

Neon concentrations measured in Siberian xenoliths are reported in Table 2. Obnazhennaya samples (n=3) range from 0.09 to 0.44 ncm^3 STP ^{20}Ne/g and Udachnaya samples (n=4) range from 0.17 to 3.22 ncm^3 STP ^{20}Ne/g. In Fig. 2, we plot all xenoliths data on a neon three-isotope diagram. The ^{20}Ne/^{22}Ne ratios range from air-like values (9.80) up to 11.35, whereas the ^{21}Ne/^{22}Ne ratios plot between the atmospheric ratio (0.029) and 0.0385 (Györe et al., 2019). All data plot between the air-DMM mixing line, defined by mid-ocean ridge popping rock 2$\prod$D43 (Moreira and Allègre, 1998), and the air-solar wind mixing trajectory (Benkert et al., 1993) (Fig. 2). The highest ^{20}Ne/^{22}Ne (11.35 $\pm$ 0.32; Siberian peridotite sample O-1104) is however significantly lower than proposed primordial mantle values (i.e., Ne-B ^{20}Ne/^{22}Ne = 12.5; Ballentine et al., 2005; solar nebula ^{20}Ne/^{22}Ne = 13.2; Williams and Mukhopadhyay, 2019).

3.3. Argon abundances and isotopes

Xenolith samples span a wide range in argon concentrations, from 165.8 to 6178 ncm^3 STP ^{40}Ar/g (Table 2). Obnazhennaya samples (n=3) range from 165.8 to 917.6 ncm^3 STP ^{40}Ar/g, whereas

Table 1
Helium and nitrogen isotope and concentration variations of Siberian mantle xenoliths.

Sample ID	Sample Wt. (g)[a] for N	Phase	$[He]_C$ ($x10^{-6}$) (cm^3 STP/g)[b]	$^3He/^4He$ (R_C/R_A)[c]	X-value[d]	$[N_2]_C$ ($x10^{-6}$) (cm^3 STP/g)	$\delta^{15}N$	$N_2/^{40}Ar$	$N_2/^{36}Ar$ ($x10^3$)	Br/Cl ($x10^{-3}$)[e]	I/Cl ($x10^{-5}$)[e]	Nitrogen Blank (%)
Obnazhennaya Peridotites												
O-1104	2.14	Cpx	1.00	4.57 ± 0.04	5340	36.0	-0.83 ± 0.14	65.7	33.8	10.0	28.3	3
O-1107	4.94	Gt	-	-	-	5.20	-3.12 ± 1.49	-				13
O-1107 (N_2 DUP)	2.601	Cpx	1.05	0.54 ± 0.01	1320	24.3	-2.28 ± 0.70	147	49.3			4
O-129/74	2.6969	Cpx	1.58	3.49 ± 0.02	632	18.8	-0.71 ± 0.76	20.5	8.70	6.25	21.3	6
O-1100	1.60	Cpx	0.08	3.67 ± 0.14	64.6	12.6	-1.49 ± 0.75	-				17
O-1106	1.32	Cpx	0.71	5.62 ± 0.08	632	23.0	-3.00 ± 0.83	-		5.52	34.1	10
Udachnaya Peridotites												
UV-98-10	3.110	Cpx	1.06	0.46 ± 0.01	881	17.9	-1.87 ± 0.76	43.1	14.3	40.3	9.4	6
UV-84-09	0.5686	Cpx	49.3	0.67 ± 0.01	37900	83.2	-5.85 ± 1.29	30.2	26.0	52.1	28.0	5
UV-33-10	-	Cpx	93.6	0.38 ± 0.01	14700	-	-	-		48.0	13.0	
UV-352-08	0.1603	Cpx	349	0.79 ± 0.01	29300	109	+3.94 ± 0.63	47.6	34.8	14.5	11.5	13
UV-367/08	2.090	Cpx	1.35	0.10 ± 0.01	8490	11.9	-3.85 ± 0.45	45.6	18.4	19.5	24.9	10
UV-39-02	3.22	Ol	-	-	-	10.5	-4.76 ± 0.66	-				6
Air				1.0			0.0	84	25.0			
Seawater				1.0			0.0	50	11.0	3.5	0.3	
DMM				8.0 ± 1.0[f]			-5.0 ± 2.0[g]	124 ± 40[h]	4600[i]	2.8 ± 0.6[j]	6.0 ± 3.0[j]	
Plume				12.0 ± 1.0[k]			+3.0 ± 2.0	74 ± 34[h]	2000[i]	2.8 ± 0.6[j]	6.0 ± 3.0[j]	
ARM				≤ 0.5			-7.0 ± 1.0	~42	~10	~55	~45	

[a] Weight of crystals loaded into crushing device and pulverized to grain size < 100 μm.
[b] Helium concentration data are corrected for air contamination where $[He]_C = ([He]_M \times (X-1))/X$. Uncertainty ± 5%.
[c] R_C/R_A notation: R_C = air-corrected sample $^3He/^4He$ ratio; R_A = atmosphere $^3He/^4He$ ratio (= 1.4 x 10^6); Air-corrected He isotope ratio = $[(R/R_A \times X)-1]/(X-1)$, where R = measured sample $^3He/^4He$ ratio. Uncertainties quoted at the 1σ level. Data from Barry et al. (2015).
[d] $X = (^4He/^{20}Ne)_M/(^4He/^{20}Ne)$air, R_M is the measured $^4He/^{20}Ne$ ratio. Dash indicates no measurable ^{20}Ne above blank.
[e] Data from Broadley et al., 2018a.
[f] Graham, 2002.
[g] Marty and Zimmermann, 1999.
[h] Marty and Dauphas, 2003.
[i] Labidi et al., 2020.
[j] Kendrick et al., 2013.
[k] Basu et al., 1995.

Table 2
Helium, neon, and argon isotope and concentration variations of Siberian mantle xenoliths.

Sample ID	Sample Wt. (g)[a] for Ne-Ar	Phase	^{40}Ar (ncm^3 STP/g)	Ar-Blank (%)	$^{40}Ar/^{36}Ar$	$^{4}He/^{40}Ar^{*}$	^{20}Ne (ncm^3 STP/g)	$^{20}Ne/^{22}Ne$	$^{21}Ne/^{22}Ne$	Ne-Blank (%)
Obnazhennaya Peridotites										
O-1104	1.5321	Cpx	548.3	1	514.3 ± 1.5	0.4	0.09	11.35 ± 0.32	0.0323 ± 0.0021	11
O-1107	-	Gt	-	-	-	-	-	-	-	-
O-1107 (N_2 DUP)	0.5221	Cpx	165.8	5	336.7 ± 0.7	66.2	0.35	10.76 ± 0.13	0.0385 ± 0.0012	6
O-129/74	1.2309	Cpx	917.6	1	424.6 ± 0.9	3.5	0.44	10.31 ± 0.11	0.0323 ± 0.0005	3
O-1100	-	Cpx			-	-	-	-	-	-
O-1106	-	Cpx			-	-	-	-	-	-
Udachnaya Peridotites										
UV-98-10	0.8847	Cpx	414.9	1	332.5 ± 0.6	11.8	0.17	11.04 ± 0.13	0.0314 ± 0.0011	10
UV-84-09	0.1659	Cpx	2754	1	860.8 ± 1.7	38.0	2.08	10.25 ± 0.11	0.0316 ± 0.0009	5
UV-33-10	0.0916	Cpx	6178	1	1121.8 ± 2.0	25.5	1.81	9.88 ± 0.12	0.0303 ± 0.0013	6
UV-352-08	0.1508	Cpx	2289	1	730.8 ± 1.2	114.6	3.22	10.25 ± 0.11	0.0303 ± 0.0006	2
UV-367/08	-	Cpx	261.0	8	403.0 ± 1.4	45.0	-	-	-	
UV-39-02	-	Ol			-	-	-	-	-	
Air					298.6			9.8	0.029	
DMM					40000[b]			12.5[c]	0.06[c]	
Plume					8000[d]			13.2[e]	0.034[e]	

[a] Weight of crystals loaded into crushing device and pulverized to grain size < 100 μm.
[b] Burnard et al., 1997.
[c] Ballentine et al., 2005.
[d] Sumino et al., 2006.
[e] Williams and Mukhopadhyay, 2019.

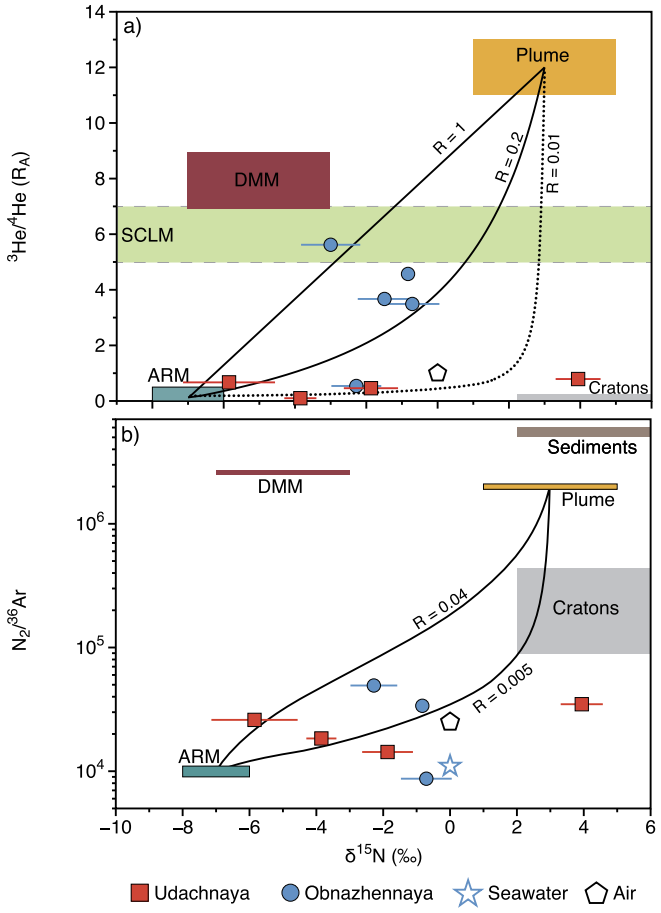

Fig. 1. He isotopes (1a), $N_2/^{36}Ar$ (1b), as a function of N isotopes. Endmember values are given in Tables 1 and 2 and described in section 4.4 along with details of the mixing model. Briefly, the model assumes an ancient radiogenic metasomatic (ARM) component that was pervasive in the S-SCLM before 360 Ma, followed by plume re-fertilization of the Obnazhennaya samples by a plume component at 250 Ma, associated with the SFB event. Uncertainties are shown to 1σ.

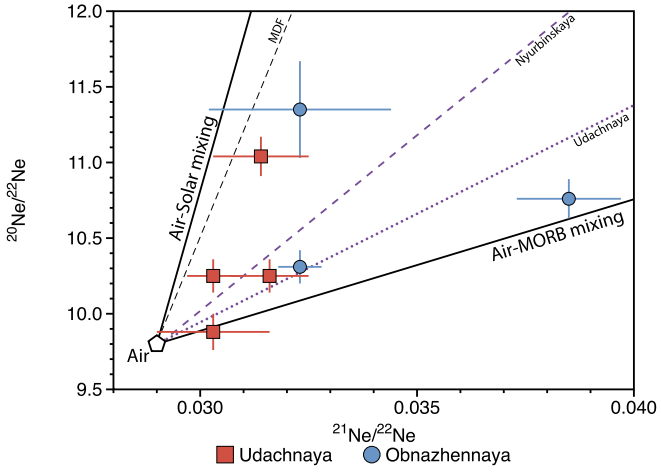

Fig. 2. Ne three isotope plot ($^{20}Ne/^{22}Ne$ vs. $^{21}Ne/^{22}Ne$). Air-Solar and Air-MORB mixing lines are superimposed atop the data. Mixing lines from two previous studies of Udachnaya olivine phenocryst (Sumino et al., 2006) and diamonds from the Nyurbinskaya kimberlite (Broadley et al., 2018b) are also shown. Ne isotope data suggest that both Obnazhennaya and Udachnaya samples contain an admixture of plume and DMM contributions. Uncertainties are shown to 1σ.

Udachnaya samples (n=5) range from 261.0 to 6178 ncm^3 STP ^{40}Ar/g. The highest argon contents are found in sample UV-33-10, which is an extremely gas-rich sample. Argon contents bracket typical concentrations from vesicular MORBs (1200×10^{-9} cm^3 STP ^{40}Ar/g; Moreira and Allègre, 1998). N_2/Ar ratios extend from 20.5 to 147 for Obnazhennaya samples and from 30.2 to 47.6 for Udachnaya samples (Table 1), therefore covering the DMM range (i.e., 84-164; Marty and Dauphas, 2003).

Argon isotope compositions ($^{40}Ar/^{36}Ar$) of the peridotite xenoliths range from 332.5 to 1122, with the highest values found in the sample with the highest ^{40}Ar concentration (Fig. S1). Obnazhennaya xenolith samples $^{40}Ar/^{36}Ar$ values range from 336.7 to 514.3. Udachnaya xenoliths $^{40}Ar/^{36}Ar$ values range from 332.5 to 1122. All measured $^{40}Ar/^{36}Ar$ values are significantly lower than DMM source (~40,000; Matsuda and Marty, 1995; Bekaert et al., 2019) and plume-source estimates (~8,000; Marty et al., 1998; Sumino et al., 2006).

4. Discussion

This suite of Siberian mantle peridotites was previously analyzed for a wide array of geochemical parameters, including major and trace elements (Howarth et al., 2014), Re-Os (Pernet-Fisher et al., 2015), He isotopes (Barry et al., 2015) and halogens (Broadley et al., 2018a). In brief, Howarth et al., 2014 showed that garnet compositions have two distinct trends in CaO–Cr_2O_3 space: increasing CaO at constant Cr_2O_3 within the harzburgite field, and decreasing CaO and Cr_2O_3 within the lherzolite field, moving from ultramafic compositions in Udachnaya toward more mafic compositions in Obnazhennaya. Pernet-Fisher et al., 2015 demonstrated that pre-plume Udachnaya peridotite xenoliths generally display unradiogenic Os-isotopes, whereas post-plume Obnazhennaya peridotites display $^{187}Os/^{188}Os$ values that overlap with the convecting mantle range. Barry et al., 2015 showed that $^3He/^4He$ values range from 0.1 to 9.8 R_A (where R_A = air $^3He/^4He$) and plot in two distinct groups: predominantly radiogenic pre-plume Udachnaya samples ($^3He/^4He = 0.41 \pm 0.30$ R_A), and 'mantle-like' post-plume Obnazhennaya samples ($^3He/^4He = 4.20 \pm 0.90$ R_A). Finally, Broadley et al., 2018a suggested that fluids within the Obnazhennaya xenoliths represent a mixture between a component rich in radiogenic ^4He, Br and I, and a component with mantle-like $^3He/^4He$ and halogen compositions. The lower $^3He/^4He$ and elevated Br/Cl and I/Cl values characteristic of Udachnaya xenoliths were considered representative of the ancient metasomatized section of the S-SCLM that was present before major influence of the SFB mantle plume. A comprehensive overview of previous findings is provided in the supplementary online material (SOM) (S.1). Here, we report new N, Ne and Ar isotope data, which are considered to be representative of mantle plume sources (section 4.2) and/or metasomatic features (section 4.3). We then present a binary mixing model (section 4.4) to explain the observed noble gas, nitrogen and halogen variations within the context of existing data.

4.1. Sample integrity

Gases released from fluid and melt inclusions within mantle-derived xenoliths are generally considered to be minimally-affected by their kimberlitic host magmas (Taylor and Anand, 2004) and/or degassing fractionation (e.g., Fischer et al., 2005), although the possibility exists that fluid inclusions can trap (air-like) fluids from kimberlitic host magmas during their ascent (Farley and Craig, 1994; Dunai and Baur, 1995). Previously, Fischer et al. (2005) showed that N isotopes measured in mineral separates from mantle xenoliths do not correlate with $^4He/^{40}Ar^*$, which is often considered a sensitive tracer of degassing due to the differing solubilities between He and Ar (Jambon et al., 1986; Colin et al., 2013). Here, $^4He/^{40}Ar^*$ values span a wide range (0.4 to 114.6), with Siberian sample values both above and below the mantle production ratio (Fig. 3). Notably, xenolith data exhibit a positive

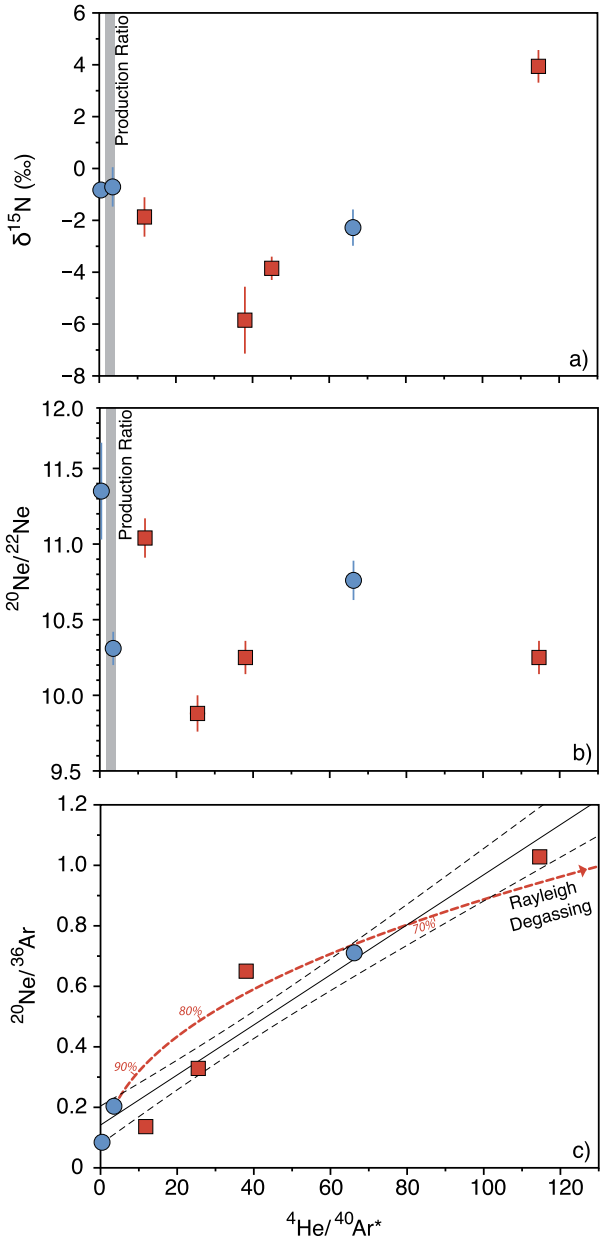

Fig. 3. N isotopes (3a), Ne isotopes (3b) and $^{20}Ne/^{36}Ar$ (3c) as a function of $^{4}He/^{40}Ar^{*}$. The lack of correlation in Fig. 3a and 3b, suggests that the isotopes of N and Ne are controlled by degassing induced fractionation and rather represent the source composition. There is a strong correlation between $^{20}Ne/^{36}Ar$ and $^{4}He/^{40}Ar^{*}$ in Fig. 3b. The data fall roughly along a solubility controlled Rayleigh degassing curve, suggesting that the noble gas elemental ratio may have been fractionation samples may have been fractionated during degassing. Rayleigh degassing equation is given in Graham, 2002 and the noble gas solubility coefficients are taken from Jambon et al., 1986. Uncertainties are shown to 1σ and are often smaller than symbol size.

correlation between $^{4}He/^{40}Ar^{*}$ and $^{20}Ne/^{36}Ar$ (Fig. 3c), which is broadly consistent with solubility controlled degassing fractionation, but could also result from mixing with a metasomatic component. Furthermore, there is no correlation between $^{4}He/^{40}Ar^{*}$ and N isotopes (Fig. 3a) or Ne isotopes (Fig. 3b), suggesting that isotopic signatures of the xenoliths have not been significantly affected by degassing fractionation.

The solubility controlled degassing curve in Fig. 3c, assumes that sample O-129-74 is most representative of the original magma given that it has a $^{4}He/^{40}Ar^{*}$ of 3.5, which is within the range of mantle $^{4}He/^{40}Ar$ production ratios (1.6 - 4.2; Graham, 2002). However, the majority of the Siberian xenoliths have $^{4}He/^{40}Ar^{*}$ values that are in excess of the mantle production ratio and are unusually high for gas extracted from xenolith fluid inclusions (Kim et al., 2005; Yamamoto et al., 2004). Fluid inclusions in xenoliths are thought to represent gases extracted early from ascending magmas, predicted to have $^{4}He/^{40}Ar^{*}$ values lower than the original magma (Moreira and Sarda, 2000). However, the high $^{4}He/^{40}Ar^{*}$ values observed in the Siberian xenoliths are more in line with residual basalts in a closed system, whereby degassing is predicted to increase the $^{4}He/^{40}Ar^{*}$ in the residual materials (e.g., Sarda and Graham, 1990) due to the higher solubility of He in the silicate melt (Jambon et al., 1986). At face value, the relationship between $^{20}Ne/^{36}Ar$ and $^{4}He/^{40}Ar^{*}$ appears more compatible with straight line mixing rather than a Rayleigh process, which would require a more curved trajectory (Fig. 3c). Furthermore, the $^{20}Ne/^{36}Ar$ of O-129-74 (Fig. 3c) is significantly lower than the mantle value (~1.2; Williams and Mukhopadhyay, 2019), suggesting that simple solubility-controlled degassing fractionation from an original mantle-like composition cannot account for the correlation between $^{4}He/^{40}Ar^{*}$ and $^{20}Ne/^{36}Ar$ (Fig. 3c). Instead, the wide range in $^{4}He/^{40}Ar^{*}$ values - above the mantle production ratio - and the correlation with $^{20}Ne/^{36}Ar$ may therefore be controlled by another process, such as mixing with a metasomatic component (see section 4.3.2).

4.2. Evidence for a mantle plume beneath the S-SCLM

4.2.1. Neon isotopes

Neon isotopes reported here are in good agreement with previously reported Ne data from Sumino et al. (2006) and Broadley et al. (2018b), who measured Ne isotopes in olivine phenocrysts and diamonds from different Siberian kimberlite pipes (Udachnaya and Nyurbinskaya), respectively, and suggested a pervasive plume contribution. Here, all Obnazhennaya and Udachnaya samples plot intermediately between DMM and plume-like endmembers in Ne three-isotope space (Fig. 2). Notably, Udachnaya samples have larger air contributions than the younger (160 Ma) Obnazhennaya samples, suggesting that the Udachnaya samples may be more strongly overprinted by the addition of atmospheric-derived Ne either during eruption, or from the introduction of atmosphere to the SCLM by subduction-related metasomatism.

The fact that plume-like Ne isotope features are observed in both suites suggests that the S-SCLM must have been influenced by plume-derived volatiles prior to the eruption of the Udachnaya suite at 360 Ma. If we assume that the same plume that formed the SFB at 250 Ma (Basu et al., 1995) imparted plume-like Ne in Udachnaya samples, then this implies that plume-lithosphere interaction occurred over a period of >100 Myr, prior to significant surface volcanism. It is possible however, that the S-SCLM has been impacted by multiple plume components throughout its history. Evidence for mantle metasomatism is also supported by He isotopes, which are as high as 9.8 R_A (Barry et al., 2015). Notably, Obnazhennaya samples presented in this study exhibit $^{3}He/^{4}He$ values up to 8.4 R_A, strongly suggesting a mantle contribution, but not necessarily a plume contribution. In contrast, Udachnaya samples are strongly radiogenic, with $^{3}He/^{4}He$ values extending as low as 0.1 R_A. Low $^{3}He/^{4}He$ in Udachnaya samples, despite plume-like Ne isotopes, suggest that Ne isotope systematics are more susceptible to overprinting by plume-driven metasomatism than He isotope systematics. This can be explained by considering the mass balance of ^{4}He in these samples; the Udachnaya suite is marked by extremely high ^{4}He concentrations (Barry et al., 2015; SOM) presumably from the radioactive decay of subducted U and Th, which makes He isotopes less susceptible to overprinting.

In summary, we show that: (1) Ne isotopes are in broad agreement with previous measurements of peridotites and diamonds

from the Udachnaya and Nyurbinskaya kimberlites (Sumino et al., 2006; Broadley et al., 2018b), and (2) both plume and DMM Ne components are present in both suites (Fig. 2), albeit to a lesser extent in Udachnaya samples. The latter observation indicates that Obnazhennaya samples experienced wholesale metasomatic overprinting, whereas Udachnaya samples were merely infiltrated by a "sniff" of plume-volatiles prior to the eruption of the SFB at 250 Ma.

4.2.2. Nitrogen isotopes

Nitrogen isotopes can potentially provide additional insights into the nature of the mantle source beneath Siberia, as DMM (-5 ± 2‰) and plumes (+3 ± 2‰) have diagnostic N isotope signatures (Dauphas and Marty, 1999). However, plume N isotope values have previously been proposed to be the direct result of recycling of surface material (Dauphas and Marty, 1999), potentially complicating this signal. Fig. 1a shows the wide range in δ^{15}N values measured in Siberian xenoliths, ranging from -5.85 ± 1.29‰ to +3.94 ± 0.63‰. Udachnaya δ^{15}N data span this entire range, whereas Obnazhennaya samples cluster around -3 to -1‰. All values fall within the broad range of what was previously reported for the SCLM (-13 to +14‰; Yokochi et al., 2009; Yamamoto et al., 2020), which is significantly larger than the accepted DMM and plume-derived δ^{15}N ranges. In Fig. 1a, we plot He isotopes (Barry et al., 2015) as a function of N isotopes (this study), together with DMM and plume mantle endmembers. It is clear from Fig. 1a that the He-N systematics of the S-SCLM cannot be explained by simple binary mixing between DMM and plume mantle components, and that an additional radiogenic ^{3}He/^{4}He component is required (see section 4.4 for details). Previously, Barry et al. (2015) suggested that this component was related to an ancient subduction-derived metasomatic event, resulting in the low ^{3}He/^{4}He values found in the Udachnaya samples. These authors speculated that subsequent addition of plume-derived volatiles to the radiogenic S-SCLM could then account for the higher ^{3}He/^{4}He measured in younger Obnazhennaya samples, which is consistent with Ne isotope observations. Assuming a plume δ^{15}N endmember of +3 ± 2‰, the range in He-N isotope data (Fig. 1a) can be explained by binary mixing (section 4.4) with a radiogenic (i.e., low ^{3}He/^{4}He) endmember marked by δ^{15}N of ≤-6‰ (Fig. 1a; Section 4.3), which we hypothesize to be subduction-derived, based on the lower ^{3}He/^{4}He ratio. Alternatively, considering the large spread of δ^{15}N values in the low ^{3}He/^{4}He Udachnaya samples, data could potentially be explained by DMM mixing with a radiogenic component marked by positive δ^{15}N (~+4‰), consistent with modern recycled sedimentary N.

In summary, the large range in δ^{15}N in peridotitic xenoliths suggests a complicated and enigmatic petrogenic and geochemical history of the S-SCLM. We conclude that N isotopes in isolation do not provide a clear picture of mantle source contributions (DMM vs. plume-derived), as data span much of the mantle range. It is however clear that the spread in data requires an additional radiogenic component, which we characterize in the following section (4.3) and hereby denote as the "Ancient Radiogenic Metasomatic" (ARM) component. In section 4.4 we use N, noble gas and halogen data to construct a comprehensive binary mixing model, accounting for the geochemical evolution of the S-SCLM since >360 Ma.

4.3. Nature of the ancient radiogenic metasomatic (ARM) component

In order to evaluate the source of N within the S-SCLM, we probe the relationship between N isotopes and halogens. In Fig. 4a and 4b, we plot Br/Cl and I/Cl as a function of N isotopes, respectively. Notably, Br/Cl and I/Cl form a negative correlation with δ^{15}N, that ranges from plume-like Br/Cl, I/Cl and δ^{15}N values towards higher Br/Cl, I/Cl and lighter N isotopic values. The high

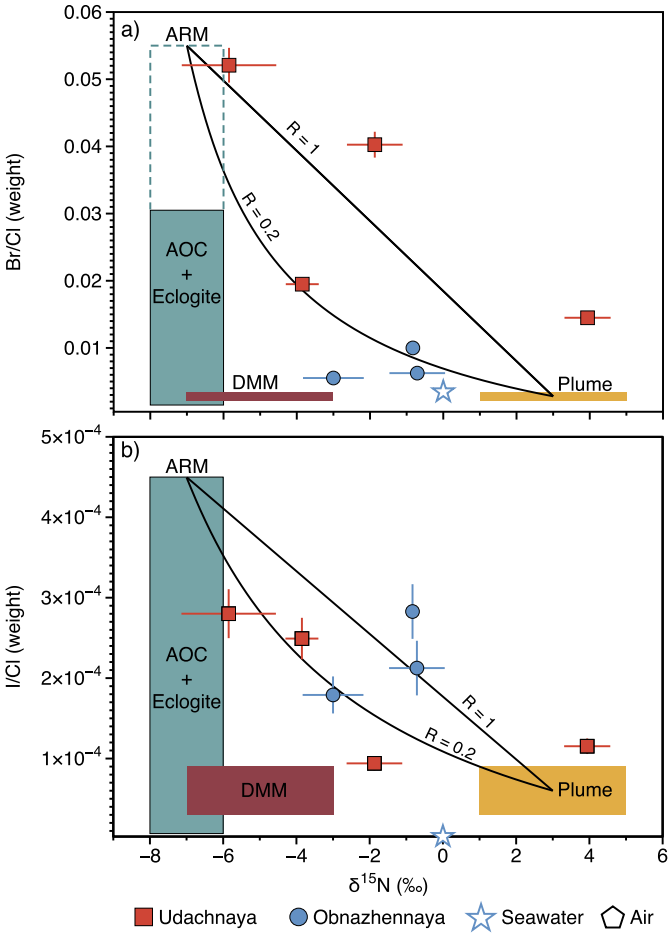

Fig. 4. Br/Cl (4a), I/Cl (4b), as a function of N isotopes. Endmember values are given in Tables 1 and 2 and described in sections 4.4 along with the details of the mixing model. The Siberian xenoliths plot between the plume mantle endmember and values similar to altered oceanic crust. The data suggests that the S-SCLM was metasomatized by an ancient radiogenic metasomatic (ARM) component prior 360 Ma. This was followed by plume re-fertilization of the Obnazhennaya samples by a plume component at 250 Ma, associated with the SFB event. Uncertainties are shown to 1σ.

Br/Cl and I/Cl values observed in the S-SCLM were previously attributed to infiltration of metasomatic fluids from subducted AOC and/or eclogite (Broadley et al., 2018a). The negative correlation between Br/Cl and I/Cl with N isotopes (Fig. 4) supports the hypothesis that light N isotopic signatures in xenoliths (i.e., the ARM component) are also derived from subduction. Notably, AOC is a major carrier of subducted N (Mitchell et al., 2010), however, the δ^{15}N isotopic signature of AOC varies widely (Li et al., 2007). The proposed ARM endmember is consistent with the ^{15}N depleted end of this range and could result from the biotic reduction of mantle-like N_2 by reaction with H_2 produced during alteration of basaltic minerals (Li et al., 2007). If true, this would implicate recycled AOC as the source of the ARM nitrogen.

4.3.1. Evidence for Archean subduction?

Strongly radiogenic He isotope signatures (Fig. 1a), coupled with high Br/Cl and I/Cl (Fig. 4) signatures in Udachnaya samples provide convincing evidence for the addition of a subducted component to the Siberian lithospheric mantle (SOM; Barry et al., 2015), however the origin of this component and the overall timing of the metasomatic event remains enigmatic. Nitrogen isotopes provide a potentially promising tool in this regard, as N-bearing sediments and AOC are considered to be recycled via subduction (Mitchell et al., 2010), potentially since the Archean

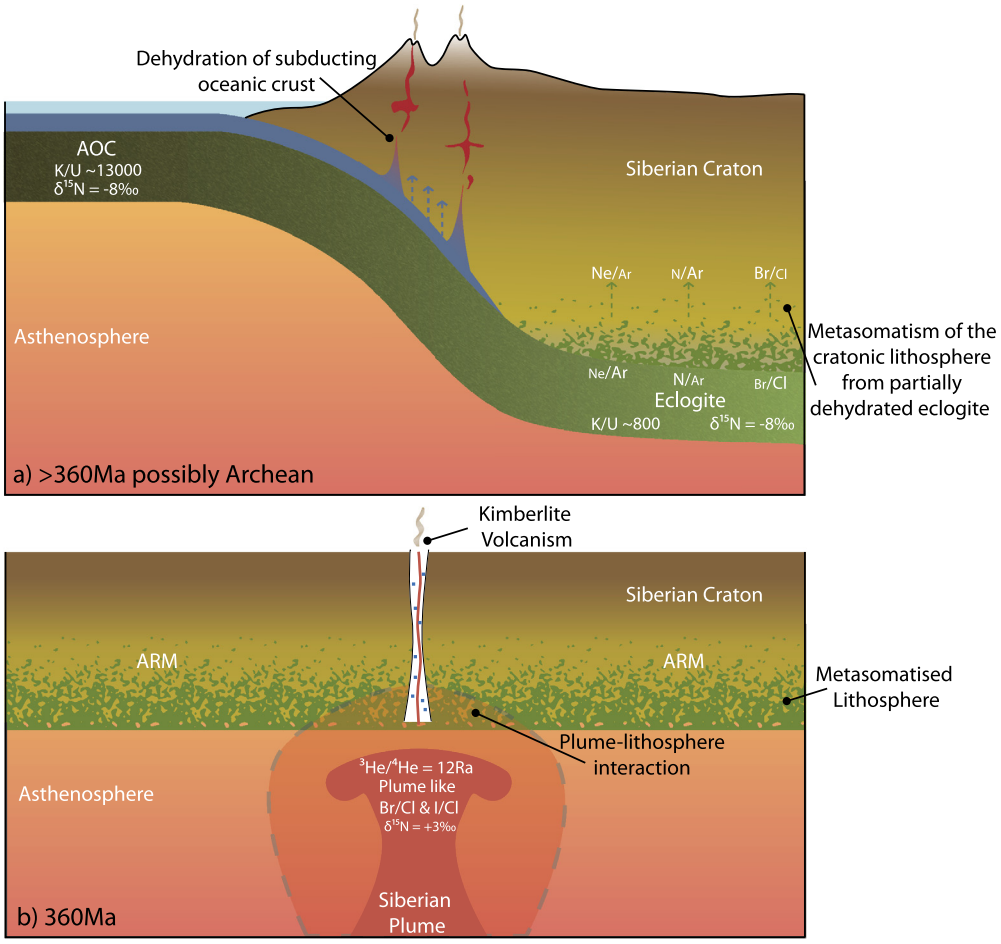

Fig. 5. Cartoon depicting the geochemical evolution of the Siberian craton. a) Prior to 360 Ma the S-SCLM was metasomatized by fluids derived from a partially dehydrated section of subducted altered oceanic crust (AOC). The light $\delta^{15}N$ values in the slab/AOC slab suggest subduction may have occurred during the Archean. Slab dehydration below the S-SCLM results in preferential release of the heavy halogens (Br and I), relative to Cl, Ne relative to Ar and N relative to Ar. b) At 360 Ma the plume - associated with the 250 Myr old SFB event - began to impinge on the S-SCLM, leading to a "sniff" of plume like volatiles in Udachnaya samples and wholesale mantle overprinting of the Obnazhennaya samples, erupted at 160 Ma.

(Marty and Dauphas, 2003). As a result, N isotopes have been used to trace subducted material in volcanic arcs (e.g., Fischer et al., 2002) and different mantle reservoirs (Dauphas and Marty, 1999; Fischer et al., 2005).

Modern sediments have an average $\delta^{15}N$ of $\sim$ +5 to +7 ‰, attributed to the kinetic isotope fractionation of N during dissimilatory denitrification of NO_3^- in the modern oxygenated oceans (Altabet and Francois, 1994). However, Archean metasediments are significantly lighter with respect to $\delta^{15}N$ than kerogens in modern sediments (Pinti et al., 2001). This is due to the fact that the N cycle in an anoxic Archean ocean would likely be dominated by chemical and metabolic reactions involving reduced forms of nitrogen (N_2, NH_3, NH_4^+), resulting in ^{15}N depleted sediments. For example, in an anoxic Archean ocean, NO_3^- would be scarce and thus dissimilatory denitrification of NO_3^- (and the associated kinetic ^{15}N enrichment) would not readily occur. Instead, the biota in the euphotic zone would directly fix N_2 or assimilate NH_4^+, leading to more negative $\delta^{15}N$ values (Marty and Dauphas, 2003) in the oceanic crust and overlying sediments. Therefore, we suggest that the ARM component could be a remnant of isotopically light subducted Archean N. This was previously hypothesized by Marty and Dauphas (2003), who showed that subduction-derived eclogitic diamonds had a distinct low $\delta^{15}N$ (-5 ‰) signature, similar to Archean organic matter. Notably, under similarly reducing conditions, low $\delta^{15}N$ values could also be produced in modern AOC (Li et al., 2007).

Pernet-Fisher et al. (2015) used Re-Os isotopes to constrain the antiquity of the metasomatic fluids; these authors demonstrated that Siberian xenoliths are a metasomatic remnant of fluids derived from a high $^{187}Re/^{188}Os$ source, such as recycled oceanic crust and/or sediments. According to Re-Os systematics, this subducted (ARM) component was introduced into the S-SCLM during craton growth events from ~1.8 to 3.0 Ga. Furthermore, Udachnaya Archean eclogite xenoliths are enriched in $\delta^{18}O$ relative to the DMM (Jacob et al., 1994), suggesting that they originate from oceanic crust that underwent extensive seawater alteration prior to subduction. Together, these ancillary pieces of evidence suggest that the subducted ARM component was originally sourced from Archean aged AOC.

4.3.2. Evolution of slab fluids during subduction

Together, halogen, N and noble gas data suggest that the S-SCLM has been metasomatized by subducted Archean AOC fluids (Fig. 5). However, we note that there are other mechanisms that could account for the non-mantle-like elemental and isotopic ratios within these samples. For example, Halama et al. (2010) measured N concentrations and $\delta^{15}N$ values in high-pressure and ultrahigh-pressure mafic eclogites and subducting AOC. They showed that, with increasing metamorphic grade, the N concentrations of eclogites decreased whilst $\delta^{15}N$ increased up to values of +8‰. The decrease was attributed to preferential loss of ^{14}N into the fluid phase (Bebout and Fogel, 1992), suggesting kinetic

fractionation occurred during generation of the fluid (Yamamoto et al., 2020). The resulting fluids released during slab dehydration would thus be isotopically lighter in δ^{15}N, in line with values measured in xenoliths samples from the mantle wedge (Yamamoto et al., 2020), which show δ^{15}N values as low as -14‰. Therefore, the low δ^{15}N value of the ARM component could, in theory, be explained by fractionation during fluid release from the subducted slab.

The dehydration of oceanic crust at subduction zones can also have a significant effect on the K and U concentrations in the released fluids and the dehydrated slab (Lassiter, 2004). Understanding how K is released from the slab can provide further insight into the behavior of N during subduction, as N in the form of NH_4^+ can readily substitute for K^+ in K-bearing minerals (Busigny and Bebout, 2013). Potassium is highly soluble in fluids generated during slab dehydration, whilst U solubility is dependent on the overall oxidation state. As a large proportion of U in the oceanic crust is in the form of insoluble U^{4+}, the K/U in the residual slab is predicted to decrease with time, whilst any released fluids will have higher K/U than the residual slab (Lassiter, 2004). This process is highlighted by the high K/U ($\geq$ 20,000) found in arc lavas and low K/U ($\sim$800) in eclogites (Fig. 5). A dehydrated slab with low K/U would therefore generate high ^{4}He/^{40}Ar*, similar to those observed in Siberian xenoliths (Fig. S2). In fact, high ^{4}He/^{40}Ar* values (similar to that measured within the Udachnaya samples) have previously been observed in subduction-related mantle xenoliths with low ^{3}He/^{4}He (Yamamoto et al., 2004; Matsumoto et al., 2005), suggesting that high (and variable) ^{4}He/^{40}Ar* in Siberian xenoliths is a feature of subduction-driven metasomatism rather than degassing. The high ^{4}He/^{40}Ar* in Udachnaya xenoliths highlight that the subducted component in the S-SCLM must have originated from a section of oceanic crust that was previously dehydrated and depleted in K, most likely during an early phase of subduction and arc magma generation. This suggests that light δ^{15}N values in the S-SCLM do not originate from fractionated fluids (Yamamoto et al., 2020), which would be marked by high K/U and therefore low ^{4}He/^{40}Ar*. The lack of any clear correlation between ^{4}He/^{40}Ar* and δ^{15}N (Fig. 3a) further supports the notion that fractionation during fluid release played a limited role in controlling the N isotopic signature of the S-SCLM. We therefore conclude that the light δ^{15}N component in the S-SCLM originates from either the subduction of Archean N or a light N component in AOC.

However, we note that the low δ^{15}N components in both modern AOC and Archean sediments are the result of reactions occurring under reducing conditions (Pinti and Hashizume, 2001; Marty and Dauphas, 2003), and therefore the two potential sources of subducted N in the S-SCLM may not be mutually exclusive. Nitrogen is stable as ammonium under subduction redox conditions (fO_2 < QFM; e.g., Mikhail et al., 2017) and behaves similarly to large ion lithophile elements, substituting for K-bearing minerals and sedimentary material. Thus, subduction of isotopically heavy NH_4^+ ($\sim$+5‰) in altered oceanic crust and sediments into the mantle may result in isotopically distinct mantle reservoirs (Sano et al., 1998; Busigny and Bebout, 2013; Halama et al., 2014). Because modern oceanic sediments are enriched in the heavy isotope of nitrogen (i.e. ^{15}N) relative to the DMM, it has been proposed that subduction of material, containing molecularly-bound nitrogen – residual to sub-arc fluid loss – could result in the introduction of heavy N-isotope signatures into the (deep) mantle (Marty and Humbert, 1997; Halama et al., 2010). N-isotope enrichments have been observed in subduction related geothermal gases (Fischer et al., 2002) and ocean island basalts (OIBs; Marty and Dauphas, 2003; Fischer et al., 2005). To date, however, such N-isotope anomalies have rarely been detected in the DMM (Marty and Zimmermann, 1999; Cartigny et al., 2001).

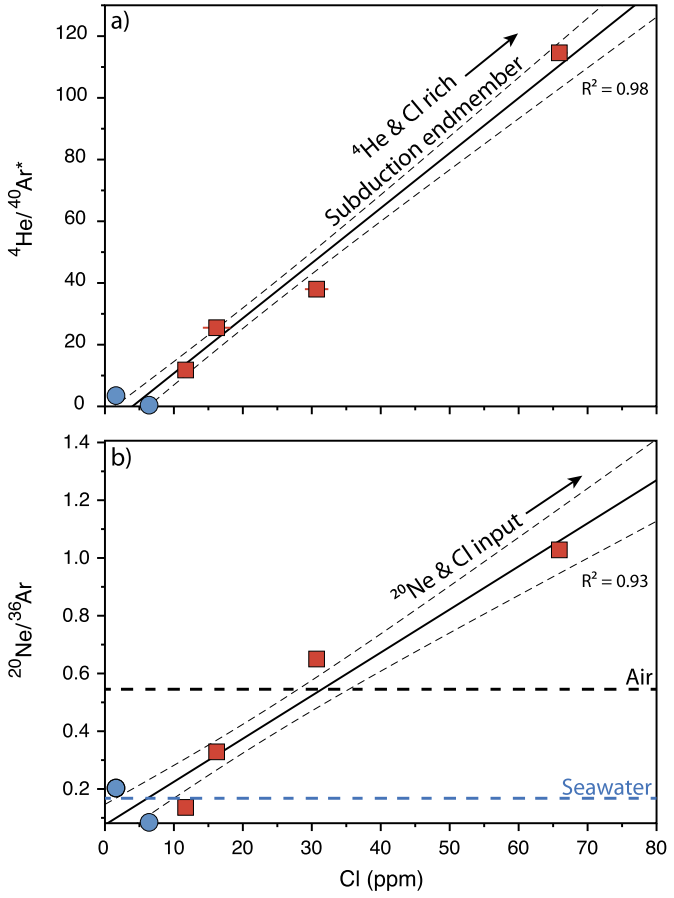

Fig. 6. (6a) ^{4}He/^{40}Ar* vs. Cl (ppm); (6b) ^{20}Ne/^{36}Ar vs. Cl (ppm). The strong positive correlation between both ^{4}He/^{40}Ar* and ^{20}Ne/^{36}Ar with Cl concentrations indicates that the noble gas elemental ratios are not a feature of degassing but are instead related to metasomatism. The correlation between ^{20}Ne/^{36}Ar and Cl indicates that the ARM endmember is enriched in Ne, relative to air and seawater indicating that Ne can be recycled to SCLM depths. The high ^{20}Ne/^{36}Ar also suggests that Ne may have been preferentially released from the slab relative to Ar, confirming that Ar is recycled to the mantle more efficiently than Ne. Uncertainties are shown to 1σ and are often smaller than symbol size.

The subducted origin of high ^{4}He/^{40}Ar* in the Siberian xenoliths is further substantiated by the strong correlation between ^{4}He/^{40}Ar* and Cl concentration (Fig. 6a). High Cl concentrations measured within the Udachnaya samples coupled with the elevated Br/Cl and I/Cl (Fig. 4), indicates that the majority of the halogens within the S-SCLM have a recycled origin. The positive correlation between ^{4}He/^{40}Ar* and Cl concentrations, therefore suggests that the high ^{4}He/^{40}Ar* measured within the xenoliths is associated with the subducted ARM component and is not a feature of degassing fractionation (Fig. 3). The positive correlation that exists between ^{20}Ne/^{36}Ar and ^{4}He/^{40}Ar* (Fig. 3c) is therefore more likely to represent mixing between the S-SCLM and a subduction-derived metasomatic component. The correlation between ^{20}Ne/^{36}Ar and Cl (Fig. 6b) suggests that the subducted (ARM) endmember has a ^{20}Ne/^{36}Ar higher than both seawater (0.17) and atmosphere (0.52). Interestingly, the ^{20}Ne/^{36}Ar of serpentinites increases from seawater-like values during dehydration and transformation to secondary peridotites (Kendrick et al., 2018). This indicates that subducting slabs can retain Ne past the point of serpentinization dehydration within the magmatic arc and deliver Ne deeper into the SCLM. However, we note that the maximum ^{20}Ne/^{36}Ar ratio measured in the Siberian xenoliths is still higher than previously measured subducting lithologies (<0.5) suggesting that at SCLM depths Ne may be preferentially released from the slab, relative to Ar, thus raising the ^{20}Ne/^{36}Ar in the ARM component and presum-

ably leaving the residual slab with low $^{20}Ne/^{36}Ar$. This implies that Ar would be preferentially retained within minerals in the subducting slab relative to Ne, and may be more efficiently transferred into the cratonic lithosphere or into the deeper mantle (Holland and Ballentine, 2006). A similar fractionation mechanism could potentially account for higher xenolith Br/Cl values relative to AOC fluids and eclogites (Fig. 4a), as Cl is considered to be preferentially subducted into the mantle relative to Br and I (Kendrick et al., 2014). Therefore, metasomatic fluids released from the slab to the S-SCLM may have enriched Br/Cl and I/Cl relative to the original AOC composition (Broadley et al., 2018a).

Finally, in Fig. 1b we show $N_2/^{36}Ar$ as a function of $\delta^{15}N$; notably, Siberian xenoliths are characterized by $N_2/^{36}Ar$ values that are significantly lower than DMM values (~2 x 10^6; Labidi et al., 2020), plume values (1.6 x 10^6; Labidi et al., 2020), cratonic endmember value (~4.5 x 10^5; Labidi et al., 2020)), sediments (~6 x 10^6; Sano et al., 1998), deep ASW (~1.1 x 10^4; Yamamoto et al., 2020), or air-values (~2.5 x 10^4). However, all data can be explained by an admixture between ARM material ($N_2/^{36}Ar$ = 1 x 10^4; $\delta^{15}N$ = -7 ± 1‰) and a plume endmember ($N_2/^{36}Ar$ = 1.6 x 10^6; $\delta^{15}N$ = +3 ± 2‰) - see model in section 4.4. The low $N_2/^{36}Ar$ of the ARM endmember suggests that ^{36}Ar is preferentially released during subduction relative to N_2, thus lowering the $N_2/^{36}Ar$ in the residual slab. The implication is that N_2 would be preferentially retained within minerals in the subducting slab relative to ^{36}Ar, and may be preferentially transferred into the cratonic lithosphere or into the deeper mantle.

4.4. Comprehensive model of S-SCLM evolution

Here we present a binary mixing model to explain new (N, Ne and Ar isotopes) and previously reported (He and halogen) data. The timing of these events can be constrained from the known eruptive history of the two Siberian pipes (Udachnaya = 360 Ma; Obnazhennaya = 160 Ma) relative to the timing of the emplacement of the SFB (250 Ma). The model assumes that the S-SCLM was initially metasomatized by ARM-like fluids (section 4.3), resulting in strongly radiogenic He and Ar signatures. Large-scale metasomatism by an ARM-like component must have occurred before the Udachnaya eruption at 360 Ma and perhaps as early as the Archean (see section 4.3.1). At 360 Ma, the Udachnaya samples erupted and retained these dominantly radiogenic He and Ar features, as well as Ne isotope evidence for a sniff of plume-derived fluids. This is likely the result of initial plume impingement, whereby Udachnaya Ne isotopes were overprinted, but He and Ar isotopes remained dominantly radiogenic due to mass balance considerations. If true, this observation implies that the plume that ultimately resulted in the SFBs may have been present below the craton, prior to 360 Ma - imparting a trace of plume-like Ne more than 100 Myr before the SFB eruption event. At 250 Ma, the SFB were emplaced on a massive scale, effectively overprinting the ARM signatures with plume-derived volatiles. Obnazhennaya samples (erupted at 160 Ma) were overwhelmed by these mantle fluids and thus shifted towards plume-like volatile compositions (Fig. 5b). Supporting evidence from additional geochemical tracers are detailed in section S.1.

This model is consistent with all noble gas, halogen and nitrogen isotope observations. In Fig. 1a, helium isotopes are plotted versus $\delta^{15}N$ values for all Siberian peridotite samples along with postulated plume ($^3He/^4He$ = 13 ± 1R_A; $\delta^{15}N$ = +3±2‰) and ARM ($^3He/^4He \leq 0.5R_A$; $\delta^{15}N$ = -7±1‰) components and binary mixing trajectories between these two endmembers. Both plume and crustal He isotope endmember values are well-constrained (Basu et al., 1995; Barry et al., 2015). The $\delta^{15}N$ values of mantle plumes are typically positive, whereas AOC is highly-variable. In this framework, we show that two-component mixing can explain coupled $\delta^{15}N$-$^3He/^4He$ systematics. As a result, Obnazhennaya samples have higher He isotopes on average and a higher $\delta^{15}N$ than the most ARM-like Udachnaya samples. Notably, all re-fertilized Obnazhennaya samples display higher than DMM $\delta^{15}N$, suggesting mixing back towards a plume-like (high $^3He/^4He$ and positive $\delta^{15}N$) source. A similar mixing model can also explain the Br/Cl (Fig. 4a) and I/Cl (Fig. 4b) variations as a function of N isotopes, whereby an initially ARM-like S-SCLM was re-fertilized at ~250 Ma - shifted He isotopes to higher values and N isotopes to less negative values, both consistent with mixing between ARM and plume-like endmember components.

5. Summary

In summary, data presented here – together with previous studies of mantle xenoliths (Kim et al., 2005; Yamamoto et al., 2004, 2020) – suggests that metasomatism of the SCLM may be a globally significant process. Critically, the metasomatic material that infiltrates the S-SCLM records an important "subduction-fingerprint" that can be used to gain insight into relative volatile element recycling efficiencies and shed light on volatile movements between Earth's surface and interior over our planet's history. We report new N and Ne-Ar isotope data for two petrologically-distinct suites of peridotitic xenoliths recovered from kimberlites that bracket the eruption of the SFB: the 360 Myr old Udachnaya and 160 Myr old Obnazhennaya pipes. We show that volatile systematics of Siberian xenoliths: (1) exhibit evidence of ancient metasomatic and/or recycled signatures - which we refer to as "Ancient Radiogenic Metasomatism" or ARM, and (2) show evidence of subsequent plume-like re-fertilization, which we attribute to the emplacement of the SFB. ARM fluids are highly enriched in radiogenic (^4He and ^{40}Ar) gases and have elevated Br/Cl and I/Cl values, consistent with an ancient subducted crustal component. The ARM component is marked by light N isotope signatures, suggesting it may be derived from an anoxic Archean subducted source. The ARM component also has high $^{20}Ne/^{36}Ar$ and low $N_2/^{36}Ar$, suggesting that Ne is preferentially released during subduction/dehydration relative to Ar, whereas Ar is preferentially released relative to N_2. This implies that in the residual slab, N_2 is most efficiently transferred to greater depths (i.e., the cratonic lithosphere and/or deep mantle), followed by Ar and finally Ne, if at all.

CRediT authorship contribution statement

Peter H. Barry: Conceptualization, Methodology, Data acquisition, Data processing, Data curation, Writing-Original draft preparation.

Michael W. Broadley: Conceptualization, Visualization, Writing-Original draft preparation.

Declaration of competing interest

The authors declare that they have no known competing financial interests or personal relationships that could have appeared to influence the work reported in this paper.

Acknowledgements

We acknowledge The National Science Foundation (NSF) awards (EAR-1144559; MGG-2015789) to PHB. We thank the late Dave Hilton and the late Larry Taylor for strong mentorship, friendship and access to their laboratories. We also thank David Bekaert, David Byrne, John Pernet-Fisher, Geoff Howarth, Ray Burgess, James Day, Sæmi Halldórsson and Sami Mikhail for fruitful discussions about these samples. We'd also like to thank the editor (Raj Dasgupta) and the two anonymous reviewers.

Appendix A. Supplementary material

Supplementary material related to this article can be found online at https://doi.org/10.1016/j.epsl.2020.116707.

References

Altabet, M.A., Francois, R., 1994. Sedimentary nitrogen isotopic ratio as a recorder for surface ocean nitrate utilization. Glob. Biogeochem. Cycles 8 (1), 103–116.

Ballentine, C.J., Marty, B., Lollar, B.S., Cassidy, M., 2005. Neon isotopes constrain convection and volatile origin in the Earth's mantle. Nature 433 (7021), 33–38.

Barry, P., Hilton, D.R., 2016. Release of subducted sedimentary nitrogen throughout Earth's mantle. Geochem. Perspect. Lett. 2 (2).

Barry, P.H., Hilton, D.R., Day, J.M., Pernet-Fisher, J.F., Howarth, G.H., Magna, T., et al., 2015. Helium isotopic evidence for modification of the cratonic lithosphere during the Permo-Triassic Siberian flood basalt event. Lithos 216, 73–80.

Basu, A.R., Poreda, R.J., Renne, P.R., Teichmann, F., Vasiliev, Y.R., Sobolev, N.V., Turrin, B.D., 1995. High-3He plume origin and temporal-spatial evolution of the Siberian flood basalts. Science 269 (5225), 822–825.

Bebout, G.E., Fogel, M.L., 1992. Nitrogen-isotope compositions of metasedimentary rocks in the Catalina Schist, California: implications for metamorphic devolatilization history. Geochim. Cosmochim. Acta 56 (7), 2839–2849.

Bekaert, D.V., Broadley, M.W., Caracausi, A., Marty, B., 2019. Novel insights into the degassing history of Earth's mantle from high precision noble gas analysis of magmatic gas. Earth Planet. Sci. Lett. 525, 115766.

Bekaert, D.V., Turner, S.J., Broadley, M.W., Barnes, J.D., Halldórsson, S.A., Labidi, J., Wade, J., Walowski, K.J., Barry, P.H., 2021. Subduction-driven volatile recycling: a global mass balance. Annu. Rev. Earth Planet. Sci. 49.

Benkert, J.P., Baur, H., Signer, P., Wieler, R., 1993. He, Ne, and Ar from the solar wind and solar energetic particles in lunar ilmenites and pyroxenes. J. Geophys. Res., Planets 98 (E7), 13147–13162.

Broadley, M.W., Ballentine, C.J., Chavrit, D., Dallai, L., Burgess, R., 2016. Sedimentary halogens and noble gases within Western Antarctic xenoliths: implications of extensive volatile recycling to the sub continental lithospheric mantle. Geochim. Cosmochim. Acta 176, 139–156.

Broadley, M.W., Barry, P.H., Ballentine, C.J., Taylor, L.A., Burgess, R., 2018a. End-Permian extinction amplified by plume-induced release of recycled lithospheric volatiles. Nat. Geosci. 11 (9), 682–687.

Broadley, M.B., Kagi, H., Burgess, R., Zedgenizov, D., Mikhail, S., Almayrac, M., et al., 2018b. Plume-lithosphere interaction, and the formation of fibrous diamonds. Geochem. Perspect. Lett.

Burnard, P., Graham, D., Turner, G., 1997. Vesicle-specific noble gas analyses of "popping rock": implications for primordial noble gases in Earth. Science 276 (5312), 568–571.

Busigny, V., Bebout, G.E., 2013. Nitrogen in the silicate Earth: speciation and isotopic behavior during mineral–fluid interactions. Elements 9 (5), 353–358.

Cartigny, P., De Corte, K., Shatsky, V.S., Ader, M., De Paepe, P., Sobolev, N.V., Javoy, M., 2001. The origin and formation of metamorphic microdiamonds from the Kokchetav massif, Kazakhstan: a nitrogen and carbon isotopic study. Chem. Geol. 176 (1–4), 265–281.

Cartigny, P., Marty, B., 2013. Nitrogen isotopes and mantle geodynamics: the emergence of life and the atmosphere–crust–mantle connection. Elements 9 (5), 359–366.

Chavrit, D., Burgess, R., Sumino, H., Teagle, D.A., Droop, G., Shimizu, A., Ballentine, C.J., 2016. The contribution of hydrothermally altered ocean crust to the mantle halogen and noble gas cycles. Geochim. Cosmochim. Acta 183, 106–124.

Colin, A., Burnard, P., Marty, B., 2013. Mechanisms of magma degassing at mid-oceanic ridges and the local volatile composition (4He–40Ar*–CO2) of the mantle by laser ablation analysis of individual MORB vesicles. Earth Planet. Sci. Lett. 361, 183–194.

Dauphas, N., Marty, B., 1999. Heavy nitrogen in carbonatites of the Kola Peninsula: a possible signature of the deep mantle. Science 286 (5449), 2488–2490.

Dunai, T.J., Baur, H., 1995. Helium, neon, and argon systematics of the European subcontinental mantle: implications for its geochemical evolution. Geochim. Cosmochim. Acta 59 (13), 2767–2783.

Farley, K.A., Craig, H., 1994. Atmospheric argon contamination of ocean island basalt olivine phenocrysts. Geochim. Cosmochim. Acta 58 (11), 2509–2517.

Fischer, T.P., Hilton, D.R., Zimmer, M.M., Shaw, A.M., Sharp, Z.D., Walker, J.A., 2002. Subduction and recycling of nitrogen along the Central American margin. Science 297 (5584), 1154–1157.

Fischer, T.P., Takahata, N., Sano, Y., Sumino, H., Hilton, D.R., 2005. Nitrogen isotopes of the mantle: insights from mineral separates. Geophys. Res. Lett. 32 (11).

Graham, D.W., 2002. Noble gas isotope geochemistry of mid-ocean ridge and ocean island basalts: characterization of mantle source reservoirs. Rev. Mineral. Geochem. 47 (1), 247–317.

Griffin, W.L., O'Reilly, S.Y., 2007. Cratonic lithospheric mantle: is anything subducted? Episodes 30 (1), 43–53.

Griffin, W.L., Shee, S.R., Ryan, C.G., Win, T.T., Wyatt, B.A., 1999. Harzburgite to lherzolite and back again: metasomatic processes in ultramafic xenoliths from the Wesselton kimberlite, Kimberley, South Africa. Contrib. Mineral. Petrol. 134 (2–3), 232–250.

Györe, D., Tait, A., Hamilton, D., Stuart, F.M., 2019. The formation of NeH+ in static vacuum mass spectrometers and re-determination of 21Ne/20Ne of air. Geochim. Cosmochim. Acta 263, 1–12.

Halama, R., Bebout, G.E., John, T., Schenk, V., 2010. Nitrogen recycling in subducted oceanic lithosphere: the record in high- and ultrahigh-pressure metabasaltic rocks. Geochim. Cosmochim. Acta 74 (5), 1636–1652.

Halama, R., Bebout, G.E., John, T., Scambelluri, M., 2014. Nitrogen recycling in subducted mantle rocks and implications for the global nitrogen cycle. Int. J. Earth Sci. 103 (7), 2081–2099.

Halldórsson, S.A., Hilton, D.R., Barry, P.H., Füri, E., Grönvold, K., 2016. Recycling of crustal material by the Iceland mantle plume: new evidence from nitrogen elemental and isotope systematics of subglacial basalts. Geochim. Cosmochim. Acta 176, 206–226.

Holland, G., Ballentine, C.J., 2006. Seawater subduction controls the heavy noble gas composition of the mantle. Nature 441 (7090), 186–191.

Holwell, D.A., Fiorentini, M., McDonald, I., Lu, Y., Giuliani, A., Smith, D.J., et al., 2019. A metasomatized lithospheric mantle control on the metallogenic signature of post-subduction magmatism. Nat. Commun. 10 (1), 1–10.

Howarth, G.H., Barry, P.H., Pernet-Fisher, J.F., Baziotis, I.P., Pokhilenko, N.P., Pokhilenko, L.N., et al., 2014. Superplume metasomatism: evidence from Siberian mantle xenoliths. Lithos 184, 209–224.

Jacob, D., Jagoutz, E., Lowry, D., Mattey, D., Kudrjavtseva, G., 1994. Diamondiferous eclogites from Siberia: remnants of Archean oceanic crust. Geochim. Cosmochim. Acta 58 (23), 5191–5207.

Jambon, A., Weber, H., Braun, O., 1986. Solubility of He, Ne, Ar, Kr and Xe in a basalt melt in the range 1250–1600 C. Geochemical implications. Geochim. Cosmochim. Acta 50 (3), 401–408.

Javoy, M., Pineau, F., Delorme, H., 1986. Carbon and nitrogen isotopes in the mantle. Chem. Geol. 57 (1–2), 41–62.

Kamo, S.L., Czamanske, G.K., Amelin, Y., Fedorenko, V.A., Davis, D.W., Trofimov, V.R., 2003. Rapid eruption of Siberian flood-volcanic rocks and evidence for coincidence with the Permian–Triassic boundary and mass extinction at 251 Ma. Earth Planet. Sci. Lett. 214 (1–2), 75–91.

Kendrick, M.A., Scambelluri, M., Honda, M., Phillips, D., 2011. High abundances of noble gas and chlorine delivered to the mantle by serpentinite subduction. Nat. Geosci. 4 (11), 807–812.

Kendrick, M.A., Arculus, R., Burnard, P., Honda, M., 2013. Quantifying brine assimilation by submarine magmas: examples from the Galápagos Spreading Centre and Lau Basin. Geochim. Cosmochim. Acta 123, 150–165.

Kendrick, M.A., Jackson, M.G., Kent, A.J., Hauri, E.H., Wallace, P.J., Woodhead, J., 2014. Contrasting behaviours of CO2, S, H2O and halogens (F, Cl, Br, and I) in enriched-mantle melts from Pitcairn and Society seamounts. Chem. Geol. 370, 69–81.

Kendrick, M.A., Scambelluri, M., Hermann, J., Padrón-Navarta, J.A., 2018. Halogens and noble gases in serpentinites and secondary peridotites: implications for seawater subduction and the origin of mantle neon. Geochim. Cosmochim. Acta 235, 285–304.

Kim, K.H., Nagao, K., Tanaka, T., Sumino, H., Nakamura, T., Okuno, M., et al., 2005. He-Ar and Nd-Sr isotopic compositions of ultramafic xenoliths and host alkali basalts from the Korean peninsula. Geochem. J. 39 (4), 341–356.

Labidi, J., Barry, P.H., Bekaert, D.V., Broadley, M.W., Marty, B., Giunta, T., et al., 2020. Hydrothermal 15 N 15 N abundances constrain the origins of mantle nitrogen. Nature 580 (7803), 367–371.

Lassiter, J.C., 2004. Role of recycled oceanic crust in the potassium and argon budget of the Earth: toward a resolution of the "missing argon" problem. Geochem. Geophys. Geosyst. 5 (11).

Li, L., Bebout, G.E., Idleman, B.D., 2007. Nitrogen concentration and δ15N of altered oceanic crust obtained on ODP Legs 129 and 185: insights into alteration-related nitrogen enrichment and the nitrogen subduction budget. Geochim. Cosmochim. Acta 71 (9), 2344–2360.

Marty, B., Dauphas, N., 2003. The nitrogen record of crust–mantle interaction and mantle convection from Archean to present. Earth Planet. Sci. Lett. 206 (3–4), 397–410.

Marty, B., Humbert, F., 1997. Nitrogen and argon isotopes in oceanic basalts. Earth Planet. Sci. Lett. 152 (1–4), 101–112.

Marty, B., Zimmermann, L., 1999. Volatiles (He, C, N, Ar) in mid-ocean ridge basalts: assessment of shallow-level fractionation and characterization of source composition. Geochim. Cosmochim. Acta 63 (21), 3619–3633.

Marty, B., Tolstikhin, I., Kamensky, I.L., Nivin, V., Balaganskaya, E., Zimmermann, J.L., 1998. Plume-derived rare gases in 380 Ma carbonatites from the Kola region (Russia) and the argon isotopic composition in the deep mantle. Earth Planet. Sci. Lett. 164 (1–2), 179–192.

Matsuda, J.I., Marty, B., 1995. The 40Ar/36Ar ratio of the undepleted mantle; a reevaluation. Geophys. Res. Lett. 22 (15), 1937–1940.

Matsumoto, T., Pinti, D.L., Matsuda, J.I., Umino, S., 2002. Recycled noble gas and nitrogen in the subcontinental lithospheric mantle: implications from N-He-Ar in fluid inclusions of SE Australian xenoliths. Geochem. J. 36 (3), 209–217.

Matsumoto, T., Morishita, T., Matsuda, J.I., Fujioka, T., Takebe, M., Yamamoto, K., Arai, S., 2005. Noble gases in the Finero phlogopite-peridotites, western Italian Alps. Earth Planet. Sci. Lett. 238 (1–2), 130–145.

Mikhail, S., Barry, P.H., Sverjensky, D.A., 2017. The relationship between mantle pH and the deep nitrogen cycle. Geochim. Cosmochim. Acta 209, 149–160.
Mitchell, E.C., Fischer, T.P., Hilton, D.R., Hauri, E.H., Shaw, A.M., de Moor, J.M., Sharp, Z.D., Kazahaya, K., 2010. Nitrogen sources and recycling at subduction zones: insights from the Izu-Bonin-Mariana arc. Geochem. Geophys. Geosyst. 11 (2).
Moreira, M., Allègre, C.J., 1998. Helium–neon systematics and the structure of the mantle. Chem. Geol. 147 (1–2), 53–59.
Moreira, M., Sarda, P., 2000. Noble gas constraints on degassing processes. Earth Planet. Sci. Lett. 176 (3–4), 375–386.
Pearson, D.G., Shirey, S.B., Carlson, R.W., Boyd, F.R., Pokhilenko, N.P., Shimizu, N., 1995. Re Os, Sm Nd, and Rb Sr isotope evidence for thick Archaean lithospheric mantle beneath the Siberian craton modified by multistage metasomatism. Geochim. Cosmochim. Acta 59 (5), 959–977.
Pernet-Fisher, J.F., Howarth, G.H., Pearson, D.G., Woodland, S., Barry, P.H., Pokhilenko, N.P., et al., 2015. Plume impingement on the Siberian SCLM: evidence from Re–Os isotope systematics. Lithos 218, 141–154.
Pernet-Fisher, J.F., Barry, P.H., Day, J.M., Pearson, D.G., Woodland, S., Agashev, A.M., Pokhilenko, L.N., Pokhilenko, N.P., 2019. Heterogeneous kimberlite metasomatism revealed from a combined He-Os isotope study of Siberian megacrystalline dunite xenoliths. Geochim. Cosmochim. Acta 266, 220–236.
Peters, K.E., Sweeney, R.E., Kaplan, I.R., 1978. Correlation of carbon and nitrogen stable isotope ratios in sedimentary organic matter 1. Limnol. Oceanogr. 23 (4), 598–604.
Pinti, D.L., Hashizume, K., 2001. 15N-depleted nitrogen in Early Archean kerogens: clues on ancient marine chemosynthetic-based ecosystems? A comment to Beaumont, V., Robert, F., 1999. Precambrian Res. 96, 62–82. Precambrian Res. 105 (1), 85–88.
Pinti, D.L., Hashizume, K., Matsuda, J.I., 2001. Nitrogen and argon signatures in 3.8 to 2.8 Ga metasediments: clues on the chemical state of the Archean ocean and the deep biosphere. Geochim. Cosmochim. Acta 65 (14), 2301–2315.
Pokhilenko, N.P., Sobolev, N.V., Kuligin, S.S., Shimizu, N., 1999. Peculiarities of distribution of pyroxenite paragenesis garnets in Yakutian kimberlites and some aspects of the evolution of the Siberian craton lithospheric mantle. In: Proceedings of the 7th International Kimberlite Conference, vol. 2. Red Roof Design, Cape Town, pp. 689–698.
Reichow, M.K., Saunders, A.D., White, R.V., Pringle, M.S., Al'Mukhamedov, A.I., Medvedev, A.I., Kirda, N.P., 2002. 40Ar/39Ar dates from the West Siberian Basin: Siberian flood basalt province doubled. Science 296 (5574), 1846–1849.
Sano, Y., Takahata, N., Nishio, Y., Marty, B., 1998. Nitrogen recycling in subduction zones. Geophys. Res. Lett. 25 (13), 2289–2292.
Sarda, P., Graham, D., 1990. Mid-ocean ridge popping rocks: implications for degassing at ridge crests. Earth Planet. Sci. Lett. 97 (3–4), 268–289.
Sharapov, V.N., Perepechko, Y.V., Perepechko, L.N., Rakhmenkulova, I.F., 2008. Mantle sources of Permian-Triassic Siberian traps (West Siberian Plate and Siberian craton). Russ. Geol. Geophys. 49 (7), 492–502.
Sobolev, S.V., Sobolev, A.V., Kuzmin, D.V., Krivolutskaya, N.A., Petrunin, A.G., Arndt, N.T., et al., 2011. Linking mantle plumes, large igneous provinces and environmental catastrophes. Nature 477 (7364), 312–316.
Sumino, H., Kaneoka, I., Matsufuji, K., Sobolev, A.V., 2006. Deep mantle origin of kimberlite magmas revealed by neon isotopes. Geophys. Res. Lett. 33 (16).
Sumino, H., Burgess, R., Mizukami, T., Wallis, S.R., Holland, G., Ballentine, C.J., 2010. Seawater-derived noble gases and halogens preserved in exhumed mantle wedge peridotite. Earth Planet. Sci. Lett. 294 (1–2), 163–172.
Taylor, L.A., Anand, M., 2004. Diamonds: time capsules from the Siberian Mantle. Geochemistry 64 (1), 1–74.
Williams, C.D., Mukhopadhyay, S., 2019. Capture of nebular gases during Earth's accretion is preserved in deep-mantle neon. Nature 565 (7737), 78–81.
Yamamoto, J., Kaneoka, I., Nakai, S.I., Kagi, H., Prikhod'ko, V.S., Arai, S., 2004. Evidence for subduction-related components in the subcontinental mantle from low 3He/4He and 40Ar/36Ar ratio in mantle xenoliths from Far Eastern Russia. Chem. Geol. 207 (3–4), 237–259.
Yamamoto, J., Takahata, N., Sano, Y., Yanagita, M., Arai, S., Prikhod'ko, V.S., 2020. Nitrogen and noble gas isotopic compositions of mantle xenoliths from Far Eastern Russia: implications for nitrogen isotopic characteristics of mantle wedge fluid. Earth Planet. Sci. Lett. 534, 116109.
Yokochi, R., Marty, B., Chazot, G., Burnard, P., 2009. Nitrogen in peridotite xenoliths: lithophile behavior and magmatic isotope fractionation. Geochim. Cosmochim. Acta 73 (16), 4843–4861.